

MIT Open Access Articles

Characterization of Adsorption Enthalpy of Novel Water-Stable Zeolites and Metal-Organic Frameworks

The MIT Faculty has made this article openly available. **Please share** how this access benefits you. Your story matters.

Citation: Kim, Hyunho, H. Jeremy Cho, Shankar Narayanan, Sungwoo Yang, Hiroyasu Furukawa, Scott Schiffres, Xiansen Li, et al. "Characterization of Adsorption Enthalpy of Novel Water-Stable Zeolites and Metal-Organic Frameworks." *Scientific Reports* 6 (January 22, 2016): 19097.

As Published: <http://dx.doi.org/10.1038/srep19097>

Publisher: Nature Publishing Group

Persistent URL: <http://hdl.handle.net/1721.1/101888>

Version: Final published version: final published article, as it appeared in a journal, conference proceedings, or other formally published context

Terms of use: Creative Commons Attribution



SCIENTIFIC REPORTS

OPEN

Characterization of Adsorption Enthalpy of Novel Water-Stable Zeolites and Metal-Organic Frameworks

Received: 16 June 2015
Accepted: 23 November 2015
Published: 22 January 2016

Hyunho Kim¹, H. Jeremy Cho¹, Shankar Narayanan¹, Sungwoo Yang¹, Hiroyasu Furukawa², Scott Schiffres¹, Xiansen Li¹, Yue-Biao Zhang², Juncong Jiang², Omar M. Yaghi² & Evelyn N. Wang¹

Water adsorption is becoming increasingly important for many applications including thermal energy storage, desalination, and water harvesting. To develop such applications, it is essential to understand both adsorbent-adsorbate and adsorbate-adsorbate interactions, and also the energy required for adsorption/desorption processes of porous material-adsorbate systems, such as zeolites and metal-organic frameworks (MOFs). In this study, we present a technique to characterize the enthalpy of adsorption/desorption of zeolites and MOF-801 with water as an adsorbate by conducting desorption experiments with conventional differential scanning calorimetry (DSC) and thermogravimetric analyzer (TGA). With this method, the enthalpies of adsorption of previously uncharacterized adsorbents were estimated as a function of both uptake and temperature. Our characterizations indicate that the adsorption enthalpies of type I zeolites can increase to greater than twice the latent heat whereas adsorption enthalpies of MOF-801 are nearly constant for a wide range of vapor uptakes.

Estimation of the adsorption enthalpy is essential for many applications including adsorption heating and cooling^{1–9}, adsorption desalination^{10–12}, and gas separation and storage systems with adsorbents^{13–15}. The adsorption enthalpy is an important parameter for modeling such systems efficiently because it dictates the energy required to operate, or the energy densities of, these systems. Due to the high enthalpy of adsorption and evaporation/condensation, and its zero global warming potential, various adsorbent-water systems have received significant attention for adsorption heating and cooling applications^{1,3–6}, as the average enthalpy of adsorption is typically higher than the latent heat of evaporation¹⁶. In addition, water capture by adsorption at low relative humidity can deliver fresh water without the use of electric power^{17,18}. The average enthalpy of adsorption is found to increase with adsorbents with IUPAC type I behavior compared to other types^{16,19}, with higher affinity to water molecules. The most studied hydrophilic adsorbents are zeolites, but recently developed metal-organic frameworks (MOFs) also have strong hydrophilic properties with stable cyclic hydrothermal performance^{17,20–23}.

The enthalpy of adsorption is most commonly estimated in either of the two following ways: estimation of the isosteric enthalpy of adsorption and direct calorimetric measurements with the use of the Tian-Calvet calorimeter¹⁹. The isosteric enthalpy of adsorption is a thermodynamic relation derived from the adsorption equilibrium measured at different temperatures with constant uptake, also known as the Clausius-Clapeyron relation, given by

$$\Delta h_{\text{isos}} = R \left(\frac{d(\ln P)}{d\left(-\frac{1}{T}\right)} \right)_{\omega} \quad (1)$$

¹Department of Mechanical Engineering, Massachusetts Institute of Technology, 77 Massachusetts Ave, Cambridge, MA 02139, United States. ²Department of Chemistry, University of California – Berkeley, Materials Sciences Division, Lawrence Berkeley National Laboratory, and Kavli Energy NanoSciences Institute at Berkeley, Berkeley, California 94720, United States. Correspondence and requests for materials should be addressed to E.W. (email: enwang@mit.edu)

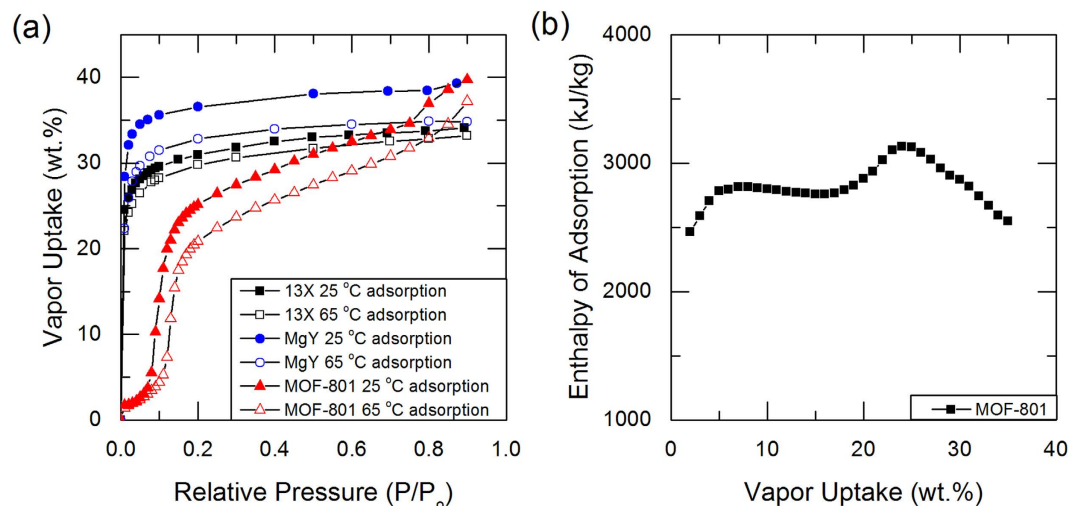


Figure 1. Adsorption isotherms and isosteric enthalpy of adsorption. (a) Adsorption isotherms (vapor uptake in weight percent vs. relative pressure, absolute pressure normalized by saturation pressure) of 13X and MgY zeolites, and MOF-801 with water pairs characterized with dynamic vapor sorption analyzer (DVS Vacuum, Surface Measurement Systems Ltd., London, UK). Adsorbents were regenerated with high vacuum (<1 Pa) with a temperature greater than 100 °C (b) Isosteric enthalpy of adsorption calculated using Eqn (1) and isotherms shown in (a) for MOF-801 and water pair with the linear interpolation method.

where Δh_{isost} , R , P , T , and ω represent the isosteric enthalpy of adsorption, universal gas constant, pressure, temperature, and vapor uptake, respectively. The isosteric enthalpy of adsorption is obtained as a function of the uptake by using Eqn (1) and adsorption isotherms measured across a wide temperature range, as shown in Fig. 1 (a). This was carried out for the MOF-801¹⁷ and water pair with a linear interpolation method, as shown in Fig. 1 (b). To use Eqn (1), we must assume ideal gas behavior in the gaseous phase, negligible volume of the adsorbed species in comparison to the gaseous phase, reversible physisorption, inertness of the adsorbent, and that thermodynamic equilibrium was reached. Adsorbents used in this study are considered to be physisorbents^{9,17,24}. Since previous studies have also shown good agreement between the isosteric method and calorimetric measurements, for N_2 and O_2 adsorbates with zeolite CaA, and CO_2 adsorbate with zeolite 13X pairs²⁵, the isosteric method is often used to characterize the differential energy for the adsorption process^{17,20,26}. However, as with many hydrophilic adsorbents, the separation between different temperature isotherms at low relative pressures (P/P_{sat} , absolute pressure over saturation pressure) is minimal, making them challenging to discern due to experimental resolution and uncertainty limitations (see Fig. 1 (a) for 13X and MgY zeolites). As such, vapor adsorption capacity obtained for 13X and MgY zeolites were 24.6wt.% and 28.4wt.% at 1% relative pressure at 25 °C, an absolute pressure near 30 Pa, shown in Fig. 1 (a), respectively. Consequently, the isosteric method is highly sensitive to the resolution of adsorption isotherms and the interpolation techniques²⁷, making calorimetric methods more suitable. However, the calorimetric method to measure the differential and the integral enthalpy of adsorption (the latter using an average enthalpy between a state 1 to 2¹⁹) requires specialized equipment^{19,28}, which is not widely available in academic and industrial facilities. In this paper, we present a new experimental technique and thermodynamic model using conventional differential scanning calorimetry (DSC) and thermogravimetric analyzer (TGA) systems that can be used to characterize the enthalpy of adsorption. With this method, we obtained the enthalpy of adsorption of water vapor for novel adsorbents, such as MgY zeolite²⁴ and MOF-801¹⁷, which can be used in a wide range of applications, including thermal energy storage, climate control, and water purification.

Results

DSC and TGA experiments. The adsorbents used in this study are 13X (molecular sieves 13X, powder, ~ 2 μ m avg. part. size, Sigma Aldrich) and MgY²⁴ zeolites, and recently reported MOF-801¹⁷. Partially saturated adsorbents at 60% relative humidity produced by mixture of nitrogen gas and deionized water vapor were prepared in a vapor sorption analyzer (Q5000SA, TA Instruments), and tested in a DSC (Discovery DSC, TA Instruments) and a TGA (Discovery TGA, TA Instruments) with various temperature ramp rates. Zeolite samples were heated up to 500 °C and MOF-801 samples were heated up to 115 °C, and temperature ramps were repeated twice during each experiment: the first for desorption heat transfer and the second for sensible heat transfer. Detailed sample preparation and experimental procedures are described in the supplementary information. With the DSC and TGA results, we defined the end of the first ramp as a dry state where no water is adsorbed in the adsorbents. Experimental data obtained from the DSC and TGA experiments with partially saturated adsorbents are shown in Fig. 2 for 13X and MgY zeolites, and MOF-801. As shown in Fig. 2 (a), the first ramps (ramp 1) have distinctly higher heat flow rates associated with latent heat compared to the second ramps (ramp 2), which were associated with sensible heat. This is expected, since the vapor desorption was carried out during the first ramp, while only the sensible heat of dry adsorbents was responsible for heat flow during the second ramp. Desorption

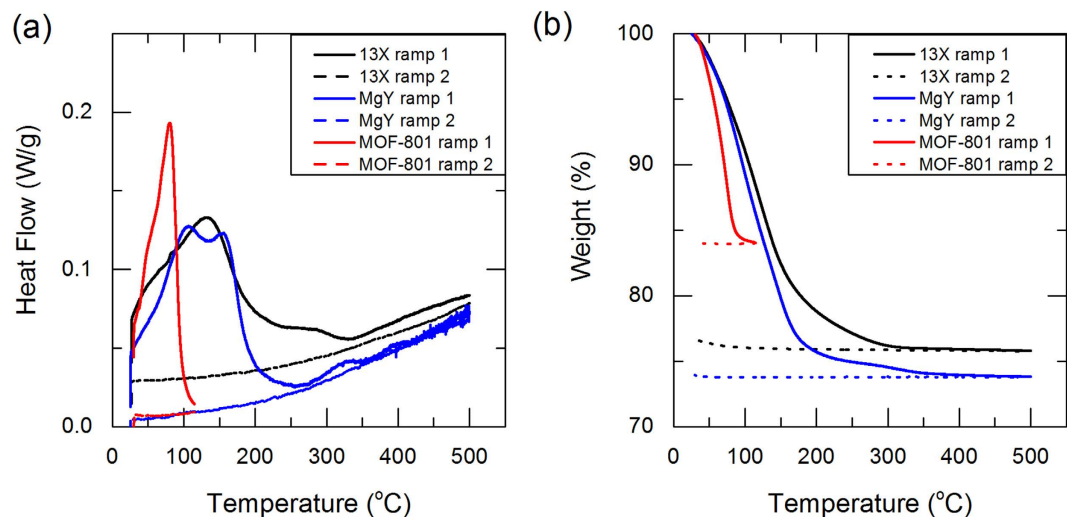


Figure 2. (a) DSC and (b) TGA results of 13X and MgY zeolites, and MOF-801 with water pairs. Data shown in this plot is obtained with 1 °C/min temperature ramp. Weights of saturated samples used in DSC experiments are 5.84 mg, 4.56 mg, and 9.37 mg for 13X, MgY, and MOF-801, respectively. Magnitude of heat flow is not important in DSC measurements as only relative heat flow between ramps 1 and 2 is considered in the calculation.

due to heating was observed up to around 350 °C for zeolites and 100 °C for MOF-801, which was observed both with DSC and TGA. The change in mass during the desorption processes (ramp 1) and the second ramp (ramp 2) was monitored with the TGA, as shown in Fig. 2 (b). From the TGA results, the vapor uptake was evaluated with the amount of mass reduced; 13X, MgY and MOF-801 were partially saturated with 31–32, 35–36, and 19–20 wt.% of water vapor, respectively. These uptake measurements were found consistent over multiple runs, as shown in Fig. 1 and Figure S2. The amount of nitrogen adsorbed at these operating conditions was also found to be negligible with the TGA, as shown in Fig. 2 (b). Measurements were repeated for 3 to 5 times in each experimental condition to obtain a 95% confidence interval from the standard error method^{29,30}.

Characterization of integral enthalpy of adsorption. We used thermodynamic analysis with the DSC and TGA measurements to determine the integral enthalpy of adsorption. In the analysis, it was assumed that the desorption kinetics in both DSC and TGA experiments are identical, assuming intra-crystalline vapor transport characteristics within adsorbent crystals in the DSC and TGA experiments are identical, and negligible pressure drop across the DSC pans due to purging flow rate. This assumption is further justified in the supplementary information (S.4 and Figure S3). A thermodynamic analysis was carried out using the DSC crucibles as the control volume (CV) and applying the simplified 1st Law of Thermodynamics for an open system (see supplementary information for details), given by

$$dE_{CV} = dQ + h_{vapor} \cdot dm_{ads} \quad (2)$$

Only the heat transfer interaction, dQ , monitored between the CV and DSC, and the vapor enthalpy flow are shown in Eqn (2), where the change in adsorbed phase mass, dm_{ads} , was monitored with the TGA. E_{CV} and h_{vapor} are the total energy within the CV and vapor enthalpy, respectively.

The overall integral enthalpy of adsorption is calculated by constructing a simple thermodynamic cycle, where an adsorbent undergoes desorption (process a-b), cool-down (process b-c), and adsorption (process c-a), as represented in Fig. 3 (a). In this approach, we consider only the heat transfer and the enthalpy flow between the environment and the CV. Processes a-b and b-c were characterized experimentally with the DSC and TGA, and process c-a is obtained by applying the 1st Law to the entire thermodynamic cycle a-b-c-a. The integral form of Eqn (2) for the desorption process, a-b, is

$$\int_a^b dE_{CV} = \int_a^b dQ + \int_a^b h_{vapor} \cdot dm_{ads} \quad (3)$$

where both the heat transfer interaction and the change in adsorbed phase mass were monitored with the DSC and TGA, respectively. Similarly for the cool-down process,

$$\int_b^c dE_{CV} = \int_b^c dQ \quad (4)$$

Heat transfer during the process is monitored with the DSC ramp 2. The 1st Law for the entire cycle is,

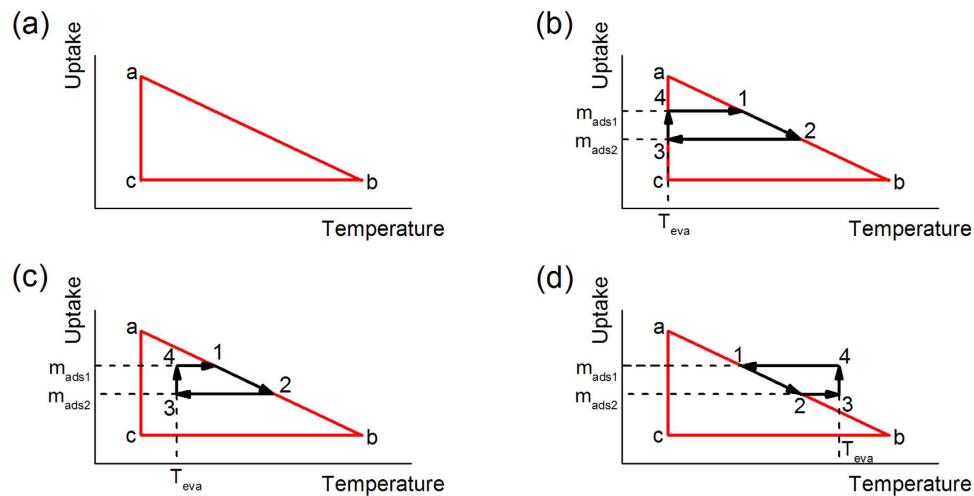


Figure 3. Thermodynamic cycle plotted in uptake vs. temperature. (a) Thermodynamic cycle representing an adsorbent undergoing desorption (process a to b), cooling down (process b to c), adsorption (process c to a) processes between temperatures T_a and T_c . (b) to (d): Subcycles within the cycle shown in (a) with various evaluation temperatures, T_{eva} . Path 1 to 2 (desorption) is carried out with DSC and TGA experiments.

$$\oint dE_{CV} = \int_a^b dE_{CV} + \int_b^c dE_{CV} + \int_c^a dE_{CV} = 0 \quad (5)$$

where the total change in energy during the cycle should sum to zero by definition of the 1st Law. Combining Eqns (2) through (5) and rearranging for process c-a, the change in the energy within the CV during the physisorption process is

$$\int_c^a dE_{CV} = -\left(\int_a^b dE_{CV} + \int_b^c dE_{CV}\right) \quad (6)$$

The change in internal energy of the CV during the isothermal process c-a is composed of both adsorbent and adsorbed vapor. However, the change in energy for the inert adsorbent is zero during the constant temperature process. For an isobaric process, $dH = dU + pdV$, where H and U are the enthalpy and internal energy, respectively. If the enthalpy of adsorption is on the same order as the latent heat of vaporization and the specific volume of the adsorbed vapor is on the same order as the liquid water, the specific integral enthalpy of adsorption, Δh_{ads} , at the initial temperature for the DSC and TGA experiments is then

$$\Delta h_{ads} = h_{vapor} - \frac{1}{m_{ads(a \rightarrow b)}} \int_c^a dE_{CV} \quad (7)$$

where h_{vapor} is the enthalpy of the vapor at room temperature (initial temperature of the DSC and TGA experiments) and $m_{ads(a \rightarrow b)}$ is the amount of the vapor desorbed during the process a-b. Δh_{ads} calculated using Eqn (7) for zeolite 13X-water pair was $3852 \pm 87 \text{ kJ/kg}_{\text{water}}$ averaged over 31–32 wt.% vapor uptake. For MgY zeolite and MOF-801, the values were $3985 \pm 150 \text{ kJ/kg}_{\text{water}}$ (averaged over 35–36 wt.% vapor uptake) and $2960 \pm 39 \text{ kJ/kg}_{\text{water}}$ (averaged over 19–20 wt.% vapor uptake), respectively. Errors reported herein are 95% confidence interval based on the standard error of characterized specific integral enthalpies of adsorption from the two different ramp rates. These values are equivalent to the average energy densities for the given adsorbent-adsorbate system, presented in Fig. 4 (a), which agrees well with direct calorimetric measurements (supplementary information).

Enthalpy of adsorption as function of uptake. We continue this analysis to estimate the enthalpy of adsorption as a function of uptake. Integration of Eqn (2) between two temperatures, T_1 and T_2 , for the desorption process, we obtain the following,

$$(m_{ads}u_{ads})_{T_2} - (m_{ads}u_{ads})_{T_1} + (U_2 - U_1)_{adsorbent} = Q_{12} + \int_1^2 h_{vapor} \cdot \frac{dm_{ads}}{dT} \cdot dT \quad (8)$$

where m_{ads} is the mass of the adsorbed vapor and $u_{ads} = (u_{ref} + c_{v,ads}T)$ is the internal energy of the adsorbed vapor, u_{ref} is the internal energy at the reference state, and $c_{v,ads}$ is the specific heat of the adsorbed vapor at constant volume. The change in the internal energy of the solid adsorbent, $(U_2 - U_1)_{adsorbent}$, is represented in Eqn (4). If a linear temperature dependence of the internal energy of the adsorbed vapor is assumed (or if the internal energy is nearly constant) between T_1 and T_2 , Eqn (8) can be represented as

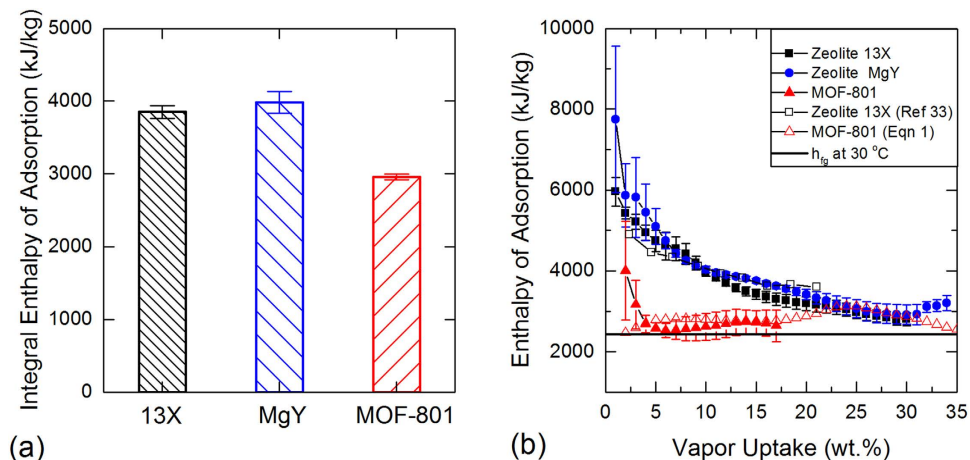


Figure 4. Characterized enthalpies of adsorption. (a) integral adsorption enthalpies and (b) adsorption enthalpies as function of vapor uptake, using Eqns (7) and (17), for 13X and MgY zeolites, and MOF-801 with water pairs at 30 °C. Integral enthalpies are averaged over 31–32 wt.%, 35–36 wt.%, and 19–20 wt.% vapor uptakes for 13X and MgY zeolites, and MOF-801, respectively. Errors reported herein are 95% confidence interval estimated from calculated adsorption enthalpies from all measurements^{29,30}. Previous calorimetric study³³ of 13X and isosteric enthalpy of MOF-801 from Fig 1(b) are also shown. (Latent heat of evaporation of water at 30 °C, $h_g = 2430$ kJ/kg).

$$u_{ads1,2}(m_{ads,T2} - m_{ads,T1}) + (U_2 - U_1)_{adsorbent} \approx Q_{12} + \int_1^2 h_{vapor} \cdot \frac{dm_{ads}}{dT} \cdot dT \quad (9)$$

with the accuracy of this equation improving with smaller temperature differences. The specific internal energy of the adsorbed vapor, $u_{ads1,2}$, between T_1 and T_2 is a both temperature- and uptake-dependent property, and the enthalpy change from the adsorbed vapor to the vapor state is then

$$\Delta h_{ads} = h_{vapor} - (u_{ads,avg} + Pv_{ads}) \quad (10)$$

If the specific volume of the adsorbed vapor, v_{ads} , is assumed to be the liquid water and Δh_{ads} is assumed to be on the same order as the latent heat of vaporization. Then Pv_{ads} is approximately 10^{-5} of Δh_{ads} . With 0.01% uncertainty, we can express a simplified Eqn (10):

$$\Delta h_{ads} = h_{vapor} - u_{ads,avg} \quad (11)$$

where Δh_{ads} is both the temperature- and uptake-dependent property

To estimate Δh_{ads} as a function of the uptake at constant temperatures, the thermodynamic cycle shown in Fig. 3 (a) is represented with smaller cycles, as shown in Fig. 3 (b–d), by choosing a temperature interval, T_1 and T_2 . Performing energy balances around the represented cycle and in the process 1 to 2, applying the 1st Law, gives

$$\int_1^2 dE_{CV} = \int_1^2 dQ + \int_1^2 h_{vapor} \cdot dm_{ads} \quad (12)$$

For the processes 2 to 3 and 4 to 1, we have,

$$\int_2^3 dE_{CV} = (U_3 - U_2)_{adsorbent} + m_{ads2}(u_{ads3} - u_{ads2}) \quad (13)$$

$$\int_4^1 dE_{CV} = (U_1 - U_4)_{adsorbent} + m_{ads1}(u_{ads1} - u_{ads4}) \quad (14)$$

where the changes in the internal energy of the solid adsorbent, $(U_3 - U_2)_{adsorbent}$ and $(U_1 - U_4)_{adsorbent}$, are known from the DSC measurements during ramp 2, equivalent to the sensible heat transfer. The mass of the adsorbed vapor within the CV is m_{ads} . The changes in the internal energy of adsorbed vapor during the processes 2 to 3 and 4 to 1, $(u_{ads3} - u_{ads2})$ and $(u_{ads1} - u_{ads4})$, are unknowns. For the process 3 to 4, an adsorption process, we have the 1st Law as shown in Eqn (15),

$$\int_3^4 dE_{CV} = m_{ads1} \cdot u_{ads4} - m_{ads2} \cdot u_{ads3} \quad (15)$$

if the linear behavior of the internal energy of the adsorbed vapor between states 3 to 4 is assumed, Eqn (15) can be simplified as

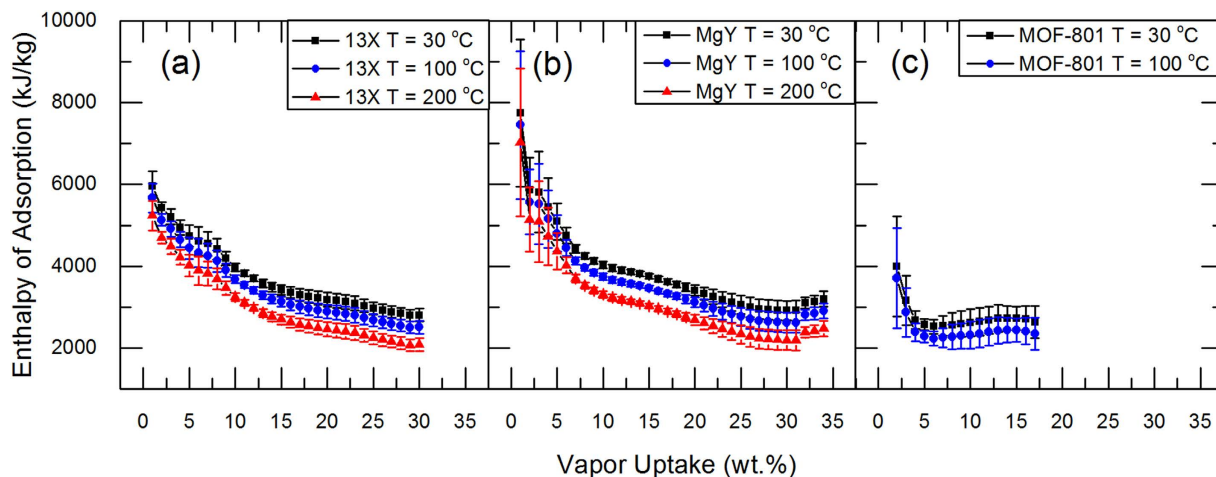


Figure 5. Enthalpies of adsorption as function of vapor uptake at various temperatures for (a) 13X and (b) MgY zeolites, and (c) MOF-801 calculated using model present in Fig. 3. Errors reported herein are 95% confidence interval estimated from calculated adsorption enthalpies from all measurements^{29,30}.

$$\int_3^4 dE_{CV} \approx u_{ads3,4}(m_{ads4} - m_{ads3}) \quad (16)$$

where $u_{ads3,4}$ is the specific integral energy of adsorbed vapor between states 3 and 4, evaluated at the constant temperature, T_{eva} . Since the net change in internal energy during a cycle is zero, by combining Eqns from (12) to (16), $u_{ads3,4}$ is

$$u_{ads3,4} = - \frac{1}{m_{ads4} - m_{ads3}} \left(\int_1^2 h_{vapor} \cdot dm_{ads} + (U_3 - U_2)_{adsorbent} + m_{ads2}(u_{ads3} - u_{ads2}) + (U_1 - U_4)_{adsorbent} + m_{ads1}(u_{ads1} - u_{ads4}) \right) \quad (17)$$

In Eqn (17), the only unknown parameter on the right-hand side is the internal energy of the adsorbed vapor. However, if the internal energy of the adsorbed vapor is assumed to match the saturated liquid water^{31,32}, we can estimate the enthalpy of adsorption as a function of the uptake, using Eqn (17) as shown in Fig. 4 (b) for 13X and MgY zeolites, and MOF-801 at 30 °C. The good agreement between the characterized enthalpy of adsorption for zeolite 13X with the previous direct calorimetric study³³ justifies this assumption. The temperature intervals used for the calculations are 15 °C for zeolites and 5 °C for MOF-801.

With the described model, estimating the enthalpy of adsorption at various temperatures by varying the evaluation temperature, T_{eva} , is possible, as shown in Fig. 3. Adsorption enthalpies evaluated at various temperatures for 13X and MgY zeolites, and MOF-801 are also obtained, as shown in Fig. 5.

Discussions

The specific integral enthalpies of adsorption with vapor for 13X and MgY zeolites, and MOF-801 were estimated by the proposed technique, as shown in Fig. 4 (a). As expected, type I zeolites have a higher average enthalpy of adsorption compared to MOF-801. Zeolites have a steep increase in the adsorption energy, greater than twice the latent heat, near the low uptake region, below 5wt.%. In contrast, MOF-801 has a nearly constant enthalpy of adsorption over a wide range of vapor uptakes, as evident in Fig. 4(b). For comparison, the isosteric enthalpy of adsorption for a MOF-801 and water pair, as shown in Fig. 1 (b), is overlaid in the same figure, showing good agreement with the results obtained by our approach.

One of the assumptions to calculate the enthalpy of adsorption using Eqn (17) is the internal energy of the adsorbed vapor being equal to the saturated liquid water. Sensitivity analysis was carried out by varying the internal energy of adsorbed vapor from being equal to the saturated liquid water and saturated vapor. This was performed by varying the adsorbed vapor-specific heat at constant volume, $c_{v,ads}$, as $du = c_{v,ads} \cdot dT$. The ice phase has a specific heat between the liquid phase and the vapor phase; therefore, this analysis provides the bounds covering all three phases and is plotted in Figure S4 (supplementary information). Variations in adsorption enthalpies by choosing different internal energies is 10–20% for zeolites and minor for MOF-801 (Figure S4) in the initial loading regime, this is in fact, our model uses the difference in internal energies between two states, the state at the evaluation temperature and the state at the actual desorption temperature. Internal energy of saturated vapor decreases beyond about 200 °C while the internal energy of liquid water continues to rise. Therefore, this variation in adsorption enthalpies becomes larger for adsorbents heated up to higher temperatures. For the purpose of characterizing the enthalpy of adsorption as a function of the uptake accurately, characterizing the specific heat/internal energy of the adsorbed vapor indeed requires using our proposed approach. However, estimating

the adsorption energy as a function of the uptake and temperature is also possible with reasonable accuracy using this approach. Likewise, calculating the overall specific integral enthalpy of adsorption using Eqn (7) does not require knowledge of the specific heat, as discussed in this paper, which also matches well with the direct calorimetric measurements (supplementary information).

With the present model, the adsorption enthalpies as a function of the vapor uptake at various temperatures were evaluated, as shown in Fig. 5. Temperatures of 30 °C, 100 °C, and 200 °C were used for zeolites, and 30 °C and 100 °C for MOF-801. Note that it is not necessary for these adsorbents to have the same vapor uptakes at the elevated temperatures. The calculated enthalpy variations due to the temperature elevations are based on the variations observed from the latent heat as a function of temperature. By preparing the partially saturated adsorbent samples with higher vapor uptakes, characterizing the adsorption enthalpies in a wider range of uptake is possible. Higher resolution and accuracy of the proposed technique can also be achieved using a DSC-TGA combined instrument. As water adsorption promises to become an important field of scientific research, the thermodynamic model and method presented in this work will serve as an important technique to characterize one of the most essential properties, enthalpy of adsorption, of various adsorbent-adsorbate systems.

References

1. Aristov, Y. I. Novel materials for adsorptive heat pumping and storage: screening and nanotailoring of sorption properties. *Journal of Chemical Engineering of Japan* **40**, 1242–1251 (2007).
2. El-Sharkawy, I. I. *et al.* Adsorption of ethanol onto phenol resin based adsorbents for developing next generation cooling systems. *International Journal of Heat and Mass Transfer* **81**, 171–178 (2015).
3. Golubovic, M. N., Hettiarachchi, H. & Worek, W. M. Sorption properties for different types of molecular sieve and their influence on optimum dehumidification performance of desiccant wheels. *International Journal of Heat and Mass Transfer* **49**, 2802–2809 (2006).
4. Henninger, S., Schmidt, F. & Henning, H.-M. Water adsorption characteristics of novel materials for heat transformation applications. *Applied thermal engineering* **30**, 1692–1702 (2010).
5. Narayanan, S., Yang, S., Kim, H. & Wang, E. N. Optimization of adsorption processes for climate control and thermal energy storage. *International Journal of Heat and Mass Transfer* **77**, 288–300 (2014).
6. Henninger, S. K., Habib, H. A. & Janiak, C. MOFs as adsorbents for low temperature heating and cooling applications. *Journal of the American Chemical Society* **131**, 2776–2777 (2009).
7. Henninger, S. K., Jeremias, F., Kummer, H. & Janiak, C. MOFs for use in adsorption heat pump processes. *European Journal of Inorganic Chemistry* **2012**, 2625–2634 (2012).
8. Narayanan, S. *et al.* Thermal battery for portable climate control. *Applied Energy* **149**, 104–116 (2015).
9. Canivet, J., Fateeva, A., Guo, Y., Coasne, B. & Farrusseng, D. Water adsorption in MOFs: fundamentals and applications. *Chemical Society Reviews* **43**, 5594–5617 (2014).
10. Ng, K. C., Thu, K., Kim, Y., Chakraborty, A. & Amy, G. Adsorption desalination: an emerging low-cost thermal desalination method. *Desalination* **308**, 161–179 (2013).
11. Thu, K., Ng, K. C., Saha, B. B., Chakraborty, A. & Koyama, S. Operational strategy of adsorption desalination systems. *International Journal of Heat and Mass Transfer* **52**, 1811–1816 (2009).
12. Wu, J. W., Hu, E. J. & Biggs, M. J. Thermodynamic cycles of adsorption desalination system. *Applied Energy* **90**, 316–322 (2012).
13. Fracaroli, A. M. *et al.* Metal-organic frameworks with precisely designed interior for carbon dioxide capture in the presence of water. *Journal of the American Chemical Society* **136**, 8863–8866 (2014).
14. Gándara, F., Furukawa, H., Lee, S. & Yaghi, O. M. High Methane Storage Capacity in Aluminum Metal-Organic Frameworks. *Journal of the American Chemical Society* **136**, 5271–5274 (2014).
15. Nguyen, N. T. *et al.* Selective Capture of Carbon Dioxide under Humid Conditions by Hydrophobic Chabazite-Type Zeolitic Imidazolate Frameworks. *Angewandte Chemie* **126**, 10821–10824 (2014).
16. Srivastava, N. & Eames, I. A review of adsorbents and adsorbates in solid-vapour adsorption heat pump systems. *Applied thermal engineering* **18**, 707–714 (1998).
17. Furukawa, H. *et al.* Water adsorption in porous metal-organic frameworks and related materials. *Journal of the American Chemical Society* **136**, 4369–4381 (2014).
18. Yang, H. *et al.* Temperature-Triggered Collection and Release of Water from Fogs by a Sponge-Like Cotton Fabric. *Advanced Materials* **25**, 1150–1154 (2013).
19. Rouquerol, J., Rouquerol, F., Llewellyn, P., Maurin, G. & Sing, K. S. *Adsorption by powders and porous solids: principles, methodology and applications*. (Academic press, 2013).
20. Küsgens, P. *et al.* Characterization of metal-organic frameworks by water adsorption. *Microporous and Mesoporous Materials* **120**, 325–330 (2009).
21. Jeremias, F., Fröhlich, D., Janiak, C. & Henninger, S. K. Water and methanol adsorption on MOFs for cycling heat transformation processes. *New Journal of Chemistry* **38**, 1846–1852 (2014).
22. Jeremias, F., Khutia, A., Henninger, S. K. & Janiak, C. MIL-100 (Al, Fe) as water adsorbents for heat transformation purposes—A promising application. *Journal of Materials Chemistry* **22**, 10148–10151 (2012).
23. Ehrenmann, J., Henninger, S. K. & Janiak, C. Water Adsorption Characteristics of MIL-101 for Heat-Transformation Applications of MOFs. *European Journal of Inorganic Chemistry* **2011**, 471–474 (2011).
24. Li, X. *et al.* Zeolite Y adsorbents with high vapor uptake capacity and robust cycling stability for potential applications in advanced adsorption heat pumps. *Microporous and Mesoporous Materials* **201**, 151–159 (2015).
25. Shen, D., Bülow, M., Siperstein, F., Engelhard, M. & Myers, A. L. Comparison of experimental techniques for measuring isosteric heat of adsorption. *Adsorption* **6**, 275–286 (2000).
26. Salame, I. I. & Bandosz, T. J. Experimental study of water adsorption on activated carbons. *Langmuir* **15**, 587–593 (1999).
27. Tedds, S., Walton, A., Broom, D. P. & Book, D. Characterisation of porous hydrogen storage materials: carbons, zeolites, MOFs and PIMs. *Faraday Discussions* **151**, 75–94, doi: 10.1039/c0fd00022a (2011).
28. Handy, B. E., Sharma, S. B., Spiewak, B. E. & Dumesic, J. A. Tian-Calvet heat-flux microcalorimeter for measurement of differential heats of adsorption. *Measurement Science and Technology* **4**, 1350 (1993).
29. Bragg, G. M. *Principles of experimentation and measurement*. (Prentice-Hall Englewood Cliffs, NJ, 1974).
30. Barry, B. A. *Errors in practical measurement in science, engineering, and technology*. (John Wiley & Sons Inc, 1978).
31. Hirasawa, Y. & Urakami, W. Study on specific heat of water adsorbed in Zeolite using DSC. *International Journal of Thermophysics* **31**, 2004–2009 (2010).
32. Chakraborty, A., Saha, B., Koyama, S. & Ng, K. Specific heat capacity of a single component adsorbent-adsorbate system. *Applied Physics Letters* **90**, 1902 (2007).
33. Gopal, R., Hollebone, B., Langford, C. & Shigeishi, R. The rates of solar energy storage and retrieval in a zeolite-water system. *Solar Energy* **28**, 421–424 (1982).

34. Wagner, W. & Pruss, A. The IAPWS Formulation 1995 for the Thermodynamic Properties of Ordinary Water Substance for General and Scientific Use. *J. Phys. Chem. Ref. Data*, **31**(2), 387–535 (2002).

Acknowledgements

The authors gratefully acknowledge the support of Advanced Research Projects Agency-Energy (ARPA-E) with Dr. Ravi Prasher and Dr. James Klausner as program managers. The authors would also like to thank the Institute for Soldier Nanotechnologies at MIT for staff help and use of equipment. H.K. acknowledges partial support from the Samsung scholarship. H.J.C. was supported by the Singapore-MIT Alliance for Research and Technology. S.S. acknowledges support from International Copper Association.

Author Contributions

H.K., S.N. and E.N.W. conceived the initial idea of this research. H.K. developed thermodynamic model, and conducted DSC and TGA experiments. H.K., H.J.C., S.N. and S.S. carried out theoretical analysis. S.Y. conducted DVS experiments. X.L. prepared MgY zeolite samples, and H.F., Y.B.Z., J.J. and O.M.Y. prepared MOF-801 samples. H.K., H.J.C., S.N. and E.N.W. were responsible for writing the paper. E.N.W. guided the work. All authors contributed on manuscript.

Additional Information

Supplementary information accompanies this paper at <http://www.nature.com/srep>

Competing financial interests: The authors declare no competing financial interests.

How to cite this article: Kim, H. *et al.* Characterization of Adsorption Enthalpy of Novel Water-Stable Zeolites and Metal-Organic Frameworks. *Sci. Rep.* **6**, 19097; doi: 10.1038/srep19097 (2016).



This work is licensed under a Creative Commons Attribution 4.0 International License. The images or other third party material in this article are included in the article's Creative Commons license, unless indicated otherwise in the credit line; if the material is not included under the Creative Commons license, users will need to obtain permission from the license holder to reproduce the material. To view a copy of this license, visit <http://creativecommons.org/licenses/by/4.0/>